

## DNA Length Dependent Photocurrent of Diketopyrrolopyrrole Aggregates Constructed with DNA

Mitsunobu Nakamura,\* Koji Tsuto, Tadao Takada, and Kazushige Yamana

Department of Materials Science and Chemistry, University of Hyogo, 2167 Shosha, Himeji, Hyogo 671-2280, Japan

**ABSTRACT:** Bis(2-thienyl)-diketopyrrolopyrrole having two Zn<sup>II</sup>-cyclens (**DPPCy**) was synthesized. DPP-aggregates were constructed by self-organization of **DPPCy** and dT<sub>n</sub>-DNAs. In the presence of L-ascorbic acid as an electron sacrifice reagent, the DPP aggregates immobilized on a gold electrode exhibit good anodic photocurrent responses as well as cathodic photocurrent responses in the presence of methyl viologen. The anodic photocurrent responses depend on the DNA lengths because of the formation of uniform DPP-aggregates corresponding to the DNA lengths. The present results show that photocurrent responses of the DPP-aggregates can be controlled by DNA lengths and electron sacrifice reagents.

Oligonucleotides are attractive molecules as construction materials for chromophore aggregates as well as for nanoarchitectures.<sup>1</sup> Using oligonucleotides, in principle, we can arrange chromophores in a defined space and distance and also control the arrangement structures via the self-assembling properties. The chromophore aggregates on oligonucleotides have been constructed by covalent<sup>2</sup> or noncovalent<sup>3</sup> approaches. Especially, the noncovalent approaches have achieved defined-length aggregations and fiber-like great length aggregations using hydrogen bonding as the driving force for the chromophore assembly. Their photonic and electronic properties, however, should await further exploration.

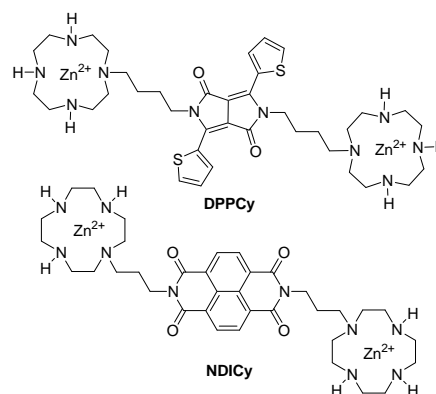
As a new strategy of the noncovalent approaches, the coordinate bonding between metal complexes with nucleobases could be anticipated as driving force. It has been well known that Zn<sup>II</sup>-cyclen complex selectively and strongly binds to thymine base disrupting a A-T base pair in double stranded DNA via the coordination of Zn<sup>II</sup> ion with the deprotonated imide nitrogen of thymine, and the hydrogen bonds between the carbonyl groups of thymine and the NH groups of cyclen.<sup>4</sup> This characteristic recognition of Zn<sup>II</sup>-cyclen has been applied to probes for DNA assays,<sup>5</sup> a cross linker,<sup>6</sup> a cleavage reagent,<sup>7</sup> and a supramolecule.<sup>8</sup> Thus, we can utilize Zn<sup>II</sup>-cyclen as the receptor unit of chromophore building blocks. Moreover, it has the advantage that the functionalization with hydrophilic Zn<sup>II</sup>-cyclen can drastically enhance the solubility of hydrophobic chromophores in aqueous solutions.

Among various chromophores, we have been interested diketopyrrolopyrrole (DPP) and 1,4,5,8-naphthalenetetracarboxylic acid diimide (NDI) chromophores because they are widely used in optoelectronic devices, such as photovoltaic cells<sup>9,10</sup> and field effect transistors.<sup>11,12</sup> Especially DPP derivatives have several advantages that they have ease of synthesis and modification, absorb visible light, and fluoresce with a high quantum yield.

Recently, we found that bis(2-thienyl)-DPP-Zn<sup>II</sup>-cyclen (**DPPCy**) and NDI-Zn<sup>II</sup>-cyclen (**NDICy**) derivatives (Chart 1) formed chromophore aggregates by self-organization with dT<sub>n</sub>-DNAs using UV-vis titrations, gel-filtration chromatography (GFC), and circular

dichroism (CD) spectroscopy.<sup>13,14</sup> UV-vis titrations of **DPPCy** (50 μM) were performed with dT<sub>n</sub>-DNAs (*n* = 10, 20, 30, 40, and 50) as a titrant. With the addition of dT<sub>n</sub>-DNA, the DPP absorption bands of **DPPCy** in the range of 420–600 nm gradually decreased, sharpened, and shifted to longer wavelength. The changes in the absorption bands indicate the formation of J-type DPP-aggregates.<sup>15</sup> In the GFC charts monitored at 260 nm and 510 nm, the mixtures of **DPPCy** and dT<sub>n</sub>-DNAs showed a unimodal peak with an eluted volume that reflected the size of the fused molecules. Moreover, induced CD signals with a positive maximum at 570 nm and a negative maximum at 505 nm were observed in the CD spectra of the mixtures of **DPPCy** and dT<sub>n</sub>-DNAs. The positive and negative CD signals were ascribed to exciton coupling among the DPP because achiral **DPPCy** itself exhibits no CD signal. These results suggest that **DPPCy** generates uniform DPP-aggregates with dT<sub>n</sub>-DNA. On the basis of UV-vis titrations, gel-filtration chromatography, and circular dichroism spectroscopy, it was also indicated that **NDICy** forms NDI-aggregates with dT<sub>n</sub>-DNAs.

**Chart 1.** Structures of bis(2-thienyl)-DPP-Zn<sup>II</sup>-cyclen and NDI-Zn<sup>II</sup>-cyclen derivatives.



The DPP-aggregates (**DPPCy-dT<sub>n</sub>**) consisting **DPPCy** and dT<sub>n</sub>-DNA exhibited photocurrent responses. The photoirradiation of the DPP-aggregates immobilized on gold electrode caused cathodic photocurrents in the presence of methyl viologen (MV<sup>2+</sup>). On the other hand, we found that the NDI-aggregates (**NDICy-dT<sub>n</sub>**) consisting **NDICy** and dT<sub>n</sub>-DNA could generate anodic photocurrents in the presence of triethanolamine.

We describe here that **DPPCy-dT<sub>n</sub>** can generate anodic photocurrent responses in the presence of L-ascorbic acid (AsA) and that the anodic photocurrent responses depend on the length of dT<sub>n</sub>-DNA.

**DPPCy-dT<sub>n</sub>** immobilized electrode was prepared as follows. The surface of gold electrode (BAS, 3 mm inner diameter) was polished

\*To whom correspondence should be addressed.  
E-mail: mitunobu@eng.u-hyogo.ac.jp

and polarized cyclically (scan rate  $150 \text{ mVs}^{-1}$ ) in the  $-0.2$  to  $+1.8 \text{ V}$  potential range in  $0.5 \text{ M H}_2\text{SO}_4$  for 10 cycles before use. The gold electrode was immersed into the buffer solution containing **DPPCy-dT<sub>n</sub>**, which was prepared using a 1:1 mixture of dT<sub>n</sub> and 3'-HS-(CH<sub>2</sub>)<sub>3</sub>-dT<sub>n</sub>,<sup>16</sup> for 3 h and then was rinsed by buffer. Photoelectrochemical measurement was carried out using an ALS 612B electrochemical analyzer in an argon-saturated buffer of pH7.6 containing  $50 \text{ mM HEPES}$ ,  $0.1 \text{ M NaNO}_3$ , and  $20 \text{ mM AsA}$  as an electron sacrifice reagent. **DPPCy-dT<sub>n</sub>** immobilized electrode was used as the working electrode along with a platinum counter electrode and an Ag/AgCl reference electrode in a three-electrode system. Photoirradiation was carried out by an Asahi Spectra MAX-302 Xe light source (300 W) with a band-pass filter.

Figure 1 shows schematic illustration of **DPPCy-dT<sub>n</sub>** immobilized electrode and photoelectrochemical responses of **DPPCy-dT<sub>10</sub>** electrode. Photoirradiation of **DPPCy-dT<sub>10</sub>** electrode using a  $560 \text{ nm}$  band pass filter caused anodic photocurrents to occur immediately in the presence of AsA. The anodic photocurrent fell down quickly with the termination of photoirradiation.

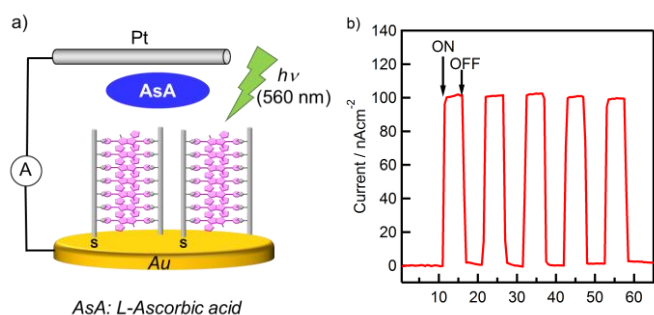


**Figure 1.** (a) Schematic illustration of DPP aggregate immobilized electrode. (b) Anodic photocurrent responses of **DPPCy-dT<sub>10</sub>** in a pH7.6 buffer containing  $20 \text{ mM AsA}$ . Photoirradiation was carried out using a  $560 \text{ nm}$  band pass filter.

The anodic photocurrent generated from **DPPCy-dT<sub>n</sub>** electrodes changed depending on the length of dT<sub>n</sub>-DNAs. Table 1 summarizes the photocurrent responses of **DPPCy-dT<sub>n</sub>** electrodes. The anodic photocurrent increased with the increase of the length of dT<sub>n</sub>-DNAs: from  $97 \pm 7.5 \text{ nA/cm}^2$  of dT<sub>10</sub> to  $210 \pm 6.8 \text{ nA/cm}^2$  of dT<sub>40</sub>. Since uniform DPP-aggregates corresponding to the length of dT<sub>n</sub>-DNAs are generated and the total amounts of Au-S bonds are almost same ( $2.1 \pm 0.3 \text{ pmol/cm}^2$ ) for each **DPPCy-dT<sub>n</sub>** electrode,<sup>17</sup> the photocurrent enhancement is probably due to the change of the total amounts of **DPPCy** on the electrode.

**Table 1.** DNA length dependence of anodic photocurrent of **DPPCy-dT<sub>n</sub>** electrodes.<sup>a</sup>

<b>DPPCy-dT<sub>n</sub></b>	Photocurrent ( $\text{nA/cm}^2$ )
<b>DPPCy-dT<sub>10</sub></b>	$97 \pm 7.5$
<b>DPPCy-dT<sub>20</sub></b>	$110 \pm 5.6$
<b>DPPCy-dT<sub>30</sub></b>	$140 \pm 15$
<b>DPPCy-dT<sub>40</sub></b>	$210 \pm 6.8$

<sup>a</sup> Photoirradiation was carried out using a  $560 \text{ nm}$  band pass filter in the presence of AsA.

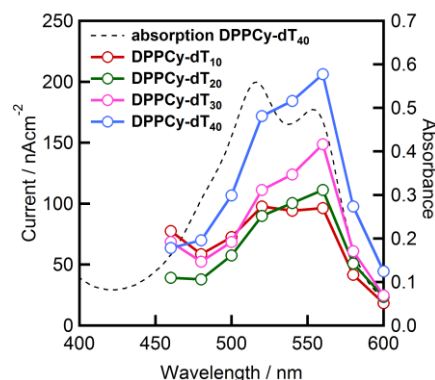


**Figure 2.** Action spectra of **DPPCy-dT<sub>n</sub>** electrodes in the region of  $460\text{--}600 \text{ nm}$ .

Figure 2 demonstrates the action spectra of **DPPCy-dT<sub>n</sub>** electrodes in the region of  $460\text{--}600 \text{ nm}$ . The action spectra of **DPPCy-dT<sub>n</sub>** electrodes are similar to the absorption spectra of **DPPCy-dT<sub>n</sub>**s in buffer solutions, indicating that the anodic photocurrent occur from the photoexcited state of **DPPCy**.

The highest occupied molecular orbital (HOMO) and lowest unoccupied molecular orbital (LUMO) levels of dimethyl-substituted bis(2-thienyl)-DPP are calculated as  $-4.96 \text{ eV}$  and  $-2.15 \text{ eV}$  by Nguyen and co-workers.<sup>18</sup> We estimated the redox potentials (vs. Ag/AgCl) of **DPPCy** (**DPPCy<sup>+</sup>/DPPCy** and **DPPCy<sup>+</sup>/DPPCy\***) using the HOMO and LUMO levels of dimethyl-substituted bis(2-thienyl)-DPP to be  $0.30 \text{ V}$  and  $-2.15 \text{ V}$  according to the method described in literature.<sup>19</sup> The redox potential of AsA (**AsA<sup>+</sup>/AsA**) is already known as  $-0.19 \text{ V}$ .<sup>20,21</sup> Therefore, the photoexcited **DPPCy** accepts an electron from AsA and the electron moves to the electrode through the DPP aggregate (Figure 3a). On the other hand, photoirradiation of **DPPCy-dT<sub>40</sub>** electrode in the presence of **MV<sup>2+</sup>** causes cathodic photocurrents.<sup>13</sup> In this system, **MV<sup>2+</sup>** accepts an electron from the photoexcited **DPPCy** to form **DPPCy<sup>+</sup>**. The generated positive hole reaches the electrode by migrating through the DPP aggregates (Figure 3b).

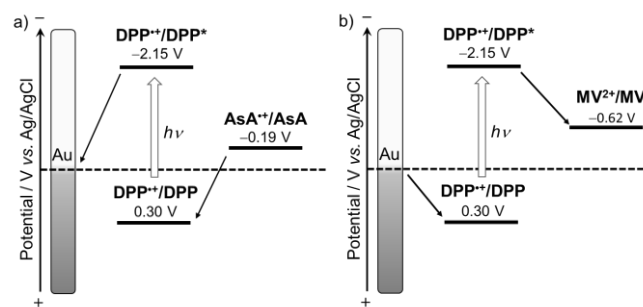


**Figure 3.** Schematic diagrams of photocurrent generation for (a) **DPPCy-dT<sub>n</sub>-AsA** system, and (b) **DPPCy-dT<sub>n</sub>-MV<sup>2+</sup>** system.

In summary, **DPPCy** forms DPP-aggregates by self-organization with dT<sub>n</sub>-DNAs. In the presence of AsA as an electron sacrifice reagent, the DPP aggregates immobilized on a gold electrode exhibit good anodic photocurrent responses as well as cathodic photocurrent responses in the presence of **MV<sup>2+</sup>**. The anodic photocurrent responses depend on the length of dT<sub>n</sub>-DNAs because of the formation of uniform DPP-aggregates corresponding to the DNA length. The results indicate that the photocurrent responses of the DPP-aggregates are controllable by DNA lengths and electron sacrifice reagents.

**KEYWORDS:** Diketopyrrolopyrrole, DNA, Self-organization, Dye aggregates, Photocurrent

Received December 10, 2014; Accepted December 22, 2014

#### ACKNOWLEDGEMENT

This work was supported by JSPS KAKENHI Grant Number 25410099.

#### REFERENCES AND NOTES

1. Rothemund, P. W. K. *Nature* **2006**, *440*, 297-302.
2. Teo, Y. N.; Kool, E. T. *Chem. Rev.* **2012**, *112*, 4221-4245.
3. González-Rodríguez, D.; Schenning, A. P. H. J. *Chem. Mater.* **2011**, *23*, 310-325.
4. Shionoya, M.; Kimura, E.; Shiro, M. *J. Am. Chem. Soc.* **1993**, *115*, 6730-6737.
5. Shiddiky, M. J. A.; Torriero, A. A. J.; Zeng, Z.; Spiccia, L.; Bond, A. M. *J. Am. Chem. Soc.* **2010**, *132*, 10053-10063.
6. Maie, K.; Nakamura, M.; Yamana, K. *Nucleosides, Nucleotides Nucleic Acids* **2006**, *25*, 453-462.
7. Tan, X.-Y.; Zhang, J.; Huang, Y.; Zhang, Y.; Zhou, L.-H.; Jiang, N.; Lin, H.-H.; Wang, N.; Xia, C.-Q.; Yu, X.-Q. *Chem. Biodiversity* **2007**, *4*, 2190-2197.
8. Aoki, S.; Zulkefeli, M.; Shiro, M.; Kimura, E. *Proc. Natl. Acad. Sci. U. S. A.* **2002**, *99*, 4894-4899.
9. Hendriks, K. H.; Li, W.; Heintges, G. H. L.; van Pruissen, G. W. P.; Wienk, M. M.; Janssen, R. A. J. *J. Am. Chem. Soc.* **2014**, *136*, 11128-11133.
10. Subramanian, S.; Earmme, T.; Murari, N. M.; Jenekhe, S. A. *Polymer Chemistry* **2014**, *5*, 5707-5715.
11. Yun, H.-J.; Kang, S.-J.; Xu, Y.; Kim, S. O.; Kim, Y.-H.; Noh, Y.-Y.; Kwon, S.-K. *Adv. Mater.* **2014**, *26*, 7300-7307.
12. Luzio, A.; Fazzi, D.; Natali, D.; Giussani, E.; Baeg, K.-J.; Chen, Z.; Noh, Y.-Y.; Facchetti, A.; Caironi, M. *Adv. Funct. Mater.* **2014**, *24*, 1151-1162.
13. Nakamura, M.; Okaue, T.; Takada, T.; Yamana, K. *Chem. Eur. J.* **2012**, *18*, 196-201.
14. Tsuto, K.; Nakamura, M.; Takada, T.; Yamana, K. *Chem. Asian J.* **2014**, *9*, 1618-1622.
15. Kirkus, M.; Wang, L.; Mothy, S.; Beljonne, D.; Cornil, J.; Janssen, R. A. J.; Meskers, S. C. J. *J. Phys. Chem. A* **2012**, *116*, 7927-7936.
16. The 3'-HS-modified dT<sub>n</sub>-DNAs were synthesized using an ABI 394 DNA/RNA Synthesizer. The synthesis was carried out in a 1.0- $\mu$ mol scale using phosphoramidites. In the synthesis, coupling was carried out using a solution of 1-*H*-tetrazole (0.5 M) in MeCN. The purification of the DNAs were performed using a reverse-phase HPLC system.
17. The total amounts of Au-S bonds for DPPCy-dT<sub>n</sub> electrodes were determined from the charge of the anodic peak of oxidative Au-S bond cleavage using cyclic voltammetry in a 0.5 M KOH solution. Widrig, C. A.; Chung, C.; Porter, M. D. *J. Electroanal. Chem. Interfacial Electrochem.* **1991**, *310*, 335-359.
18. Tamayo, A. B.; Tantiwiwat, M.; Walker, B.; Nguyen, T.-Q. *J. Phys. Chem. C* **2008**, *112*, 15543-15552.
19. Trasatti, S. *Pure Appl. Chem.* **1986**, *58*, 955-966.
20. Imahori, H.; Azuma, T.; Ajavakom, A.; Norieda, H.; Yamada, H.; Sakata, Y. *J. Phys. Chem. B* **1999**, *103*, 7233-7237.
21. Liu, Y.-F.; Chen, J.-X.; Xu, M.-Q.; Zhao, G.-C. *Int. J. Electrochem. Sci.* **2014**, *9*, 4014-4023.